

Axisymmetric buckling of the circular annular nanoplates using finite difference method

M.R. Karamooz Ravari · A.R. Shahidi

Received: 5 September 2011 / Accepted: 31 July 2012 / Published online: 10 August 2012
© Springer Science+Business Media B.V. 2012

Abstract In recent years nanostructures have been used in a vast number of applications, so the study of the mechanical behavior of such structures could be of interest. In the present study, the buckling behavior of circular annular plates and solid disks under uniform compression has been surveyed for several combinations of boundary conditions using the finite difference method. The affects of nonlocal parameter and the plate size have been studied for each combination of boundary conditions. The obtained results are in good agreement with the other studies and the reality. The results also convince that the finite difference method is a powerful method for solving the problems corresponding to nanoplate mechanical behaviors.

Keywords Nanoplate · Buckling load · Finite difference method · Circular annular plates · Solid disks · Half-intenerated grid

1 Introduction

Nanostructures have a wide range of applications due to their superior mechanical, thermal and electrical properties. These properties let to produce small devices that were impossible before.

There are two approaches for mechanical analysis of nanoscale structures namely molecular dynamic model and continuum models. It is shown in many studies that continuum models can be used effectively in the analysis of nano structures [1].

In recent years many efforts were concentrated on the studying of mechanical behaviors of nanostructures. These studies could be classified in two experimental and theoretical groups. Since controlling of the experiment conditions is not easy in the nano scale so the theoretical methods is in important.

Liu and Rajapakse [2] developed a general model to analyze the behavior of nanobeams with arbitrary cross sections using Gurtin's continuum surface theory based on Euler–Bernoulli and Timoshenko beam models. Wang and Feng [3] studied the stability and vibration of nanowires by using Timoshenko beam theory. Farshi et al. [4] studied the size dependent vibration of nanotubes using a modified beam theory based on Timoshenko beam. Fuand Zhang [5] used analog equation method to solve the problem of electrically actuated nanobeams with consideration of surface. Fu et al. [6] studied the affects of the surface energies on nonlinear bending and vibration of nanobeams. J.N. Sharma et al. [7] derived the closed form expressions for the transverse vibrations of a homogeneous isotropic, thermoelastic thin beam with voids, based on Euler–Bernoulli theory. They also studied the effects of voids, relaxation times, thermomechanical coupling, surface conditions and beam dimensions on energy dissipation

M.R. Karamooz Ravari (✉) · A.R. Shahidi
Department of Mechanical Engineering, Isfahan University
of Technology, 84156-83111, Isfahan, Iran
e-mail: m.karamoozravari@me.iut.ac.ir

induced by thermoelastic damping in MEMS/NEMS resonators for beams under clamped and simply supported boundary conditions. B. Bar-On et al. [8] studied the effects of surface residual stresses on nano-beams including mid-plane stretching under near resonance vibrations. In another work [9], they analyzed the deflection of clamped nano-beam due to stochastic surface stresses, induced by adsorption/desorption of surrounding particles. They considered both linear and non-linear effects using 1D nano-beam model. A. Tylikowski [10] studied the stochastic parametric vibrations of micro- and nano-rods based on Eringen's nonlocal elasticity theory and Euler–Bernoulli beam theory. B. Mohammadi et al. [11] presented an efficient numerical method to analyze the vibration behavior of nano Timoshenko beams based on Eringen's nonlocal elasticity theory. Yan-Gao Hu et al. [12] presented a brief review of vibrations of single-walled carbon nanotubes (SWCNTs) using the nonlocal beam model and nonlocal rod model and MD simulation. Yang Yang et al. [13] simulated the double-walled carbon nanotubes with a Timoshenko beam model based on the nonlocal continuum elasticity theory, referred to as an analytically nonlocal Timoshenko-beam (ANT) model. Lu et al. [14] studied the effect of additional surface properties illustrating the size dependent mechanical behavior of nanoplates using generalized Kirchhoff and Mindlin plate theories. Sheng et al. [15] analyzed the three dimensional elasticity of nanoplates including surface properties using the theory of laminated structures. Assadi et al. [16] used the laminated plate theory to survey the effects of surface properties on the dynamic behavior of nanoplates in thermal environments using size dependent Young's modulus. S. Narendar et al. [17] studied the thermal effects on the ultrasonic wave propagation characteristics of a nanoplate based on the nonlocal continuum theory. B. Arash et al. [18] provided a comprehensive study on wave propagations in SLGSs by a developed nonlocal finite element plate model and MD simulations. They also studied the effect of the size of the sheet width on GS phonon dispersion relations. Assadi et al. [19] studied the transverse vibration of circular nanoplates with consideration of surface energies and obtained the size dependent natural frequencies and vibration mode shapes. Behfar et al. [20] used classical continuum modeling for vibration of multilayered graphene sheet embedded in an elastic medium. Murmu et al. [21, 22] studied the size dependent vi-

bration of nanoplates using nonlocal continuum theory. R.M. Lin [23] proposed a continuum-based plate model to study the nanoscale vibration characteristics of multi-layered graphene sheets (MLGSs). Generalized Differential Quadrature (GDQ) method was used to predict the natural frequencies and their associated vibration modes of single-layered and triple-layered graphene sheets, as well as general MLGSs. Huang [24] studied size dependent bending, buckling and vibration of nanoplates by using the nonlinear Kirchhoff plate theory and Von-Karman nonlinearity assumptions. Tolga Aksencer et al. [1] presented the Levy type solution method for vibration and buckling of nanoplates using nonlocal elasticity theory. Babaei et al. [25] studied buckling of the quadrilateral nanoplates by using of nonlocal plate theory. Pradhan et al. [26] analyzed the buckling of rectangular single-layered graphene sheets under biaxial compression by using the nonlocal elasticity. Sakhaee-Pour [27] studied the buckling of graphene nanosheets with atomistic modeling. S. Narendar [28] studied the buckling analysis of isotropic nanoplates using the two variable refined plate theory and nonlocal small scale effects. A. Farajpour et al. [29] studied axisymmetric buckling of the circular graphene sheets using the nonlocal continuum plate model. Nabian et al. [30] studied the pull-in instability of circular micro-scale plates under uniform hydrostatic and non-uniform electrostatic pressures.

Nanoplates are widely used in MEMS/NEMS components so the buckling of them is in important. In this paper first governing differential equation has been introduced according to literature and then this equation has been solved using finite difference method to obtain the non-dimensional buckling load for several combinations of boundary conditions. In these cases suitable grids have been presented to repel the singularity of the solid disk at its center. The obtained results have been compared with those from literature for solid disk and have been discussed for circular annular one. The results show the finite difference method could be used as a powerful method for solving such problems.

2 Nonlocal plate model

The stress equation for a linear homogeneous nonlocal elastic body by neglecting the body force using nonlocal elasticity theory [31] can be written as

$$\sigma_{ij}(x) = \int \lambda(|x - x'|, \alpha) c_{ijkl} \varepsilon_{kl}(x') dV(x') \quad \forall x \in V \tag{1}$$

Here σ_{ij} , ε_{ij} and C_{ijkl} are the stress, strain and fourth order elasticity tensors, respectively. $\lambda(|x - x'|, \mu)$ is the non-local modulus, $|x - x'|$ represents the distance in Euclidean form and μ is a material constant ($\mu = e_0 a / \ell$) that depends on the internal (lattice parameter, granular size, distance between C–C bonds), a and external characteristics lengths (crack length, wave length), ℓ . The parameter e_0 is estimated such that the relations of the non-local elasticity model could provide satisfied approximation of atomic dispersion curves of plane waves with those of atomic lattice dynamics.

Since solving integral constitutive is difficult, a simplified equation in differential form of Eq. (1) is used as a basis of all non-local constitutive formulation:

$$(1 - \mu^2 \ell^2 \nabla^2) \sigma = C : \varepsilon \tag{2}$$

Here “:” represents the double dot product. $\nabla^2 = (\partial^2 / \partial x^2 + \partial^2 / \partial y^2)$ is the Laplacian operator. Using Laplacian operator the two-dimensional non-local constitutive relation can be expressed as:

$$\sigma_{xx} - (e_0 a)^2 \nabla^2 \sigma_{xx} = \frac{E}{(1 - \nu^2)} (\varepsilon_{xx} + \nu \varepsilon_{yy}) \tag{3a}$$

$$\sigma_{yy} - (e_0 a)^2 \nabla^2 \sigma_{yy} = \frac{E}{(1 - \nu^2)} (\varepsilon_{yy} + \nu \varepsilon_{xx}) \tag{3b}$$

$$\tau_{xy} - (e_0 a)^2 \nabla^2 \tau_{xy} = G \gamma_{xy} \tag{3c}$$

Stress resultants in the Cartesian coordinate can be written as:

$$N_{xx} = \int_{-t/2}^{t/2} \sigma_{xx} dz, \quad N_{yy} = \int_{-t/2}^{t/2} \sigma_{yy} dz \tag{4a}$$

$$N_{xy} = \int_{-t/2}^{t/2} \sigma_{xy} dz$$

$$M_{xx} = \int_{-t/2}^{t/2} z \sigma_{xx} dz, \quad M_{yy} = \int_{-t/2}^{t/2} z \sigma_{yy} dz \tag{4b}$$

$$M_{xy} = \int_{-t/2}^{t/2} z \sigma_{xy} dz$$

Using Eqs. (3a)–(3c) and (4a)–(4b) one obtains the following non-local constitutive relation based on classical plate’s theory:

$$N_{xx} - (e_0 a)^2 \left(\frac{\partial^2 N_{xx}}{\partial x^2} + \frac{\partial^2 N_{xx}}{\partial y^2} \right) = C \left(\frac{\partial u}{\partial x} + \nu \frac{\partial v}{\partial y} \right) \tag{5a}$$

$$N_{yy} - (e_0 a)^2 \left(\frac{\partial^2 N_{yy}}{\partial x^2} + \frac{\partial^2 N_{yy}}{\partial y^2} \right) = C \left(\frac{\partial v}{\partial y} + \nu \frac{\partial u}{\partial x} \right) \tag{5b}$$

$$N_{xy} - (e_0 a)^2 \left(\frac{\partial^2 N_{xy}}{\partial x^2} + \frac{\partial^2 N_{xy}}{\partial y^2} \right) = C \frac{(1 - \nu)}{2} \left(\frac{\partial u}{\partial y} + \frac{\partial v}{\partial x} \right) \tag{5c}$$

$$M_{xx} - (e_0 a)^2 \left(\frac{\partial^2 M_{xx}}{\partial x^2} + \frac{\partial^2 M_{xx}}{\partial y^2} \right) = -D \left(\frac{\partial^2 w}{\partial x^2} + \nu \frac{\partial^2 w}{\partial y^2} \right) \tag{5d}$$

$$M_{yy} - (e_0 a)^2 \left(\frac{\partial^2 M_{yy}}{\partial x^2} + \frac{\partial^2 M_{yy}}{\partial y^2} \right) = -D \left(\frac{\partial^2 w}{\partial y^2} + \nu \frac{\partial^2 w}{\partial x^2} \right) \tag{5e}$$

$$M_{xy} - (e_0 a)^2 \left(\frac{\partial^2 M_{xy}}{\partial x^2} + \frac{\partial^2 M_{xy}}{\partial y^2} \right) = -D(1 - \nu) \left(\frac{\partial^2 w}{\partial x \partial y} \right) \tag{5f}$$

Here $D = \frac{Et^3}{12(1 - \nu^2)}$, $C = \frac{Et}{(1 - \nu^2)}$, E is elastic modulus, ν is Poisson’s ratio, t is plate thickness, w is out-of-plane displacement.

Note that stress resultants displacement relations given in Eqs. (5a)–(5f); reduce to that of the classical relation when the scale coefficient $e_0 a$ is set to zero.

Using the principle of virtual work, the following equilibrium equations can be obtained:

$$\frac{\partial N_{xx}}{\partial x} + \frac{\partial N_{xy}}{\partial y} = m_0 \frac{\partial^2 u}{\partial t^2} \tag{6a}$$

$$\frac{\partial N_{yy}}{\partial y} + \frac{\partial N_{xy}}{\partial x} = m_0 \frac{\partial^2 v}{\partial t^2} \tag{6b}$$

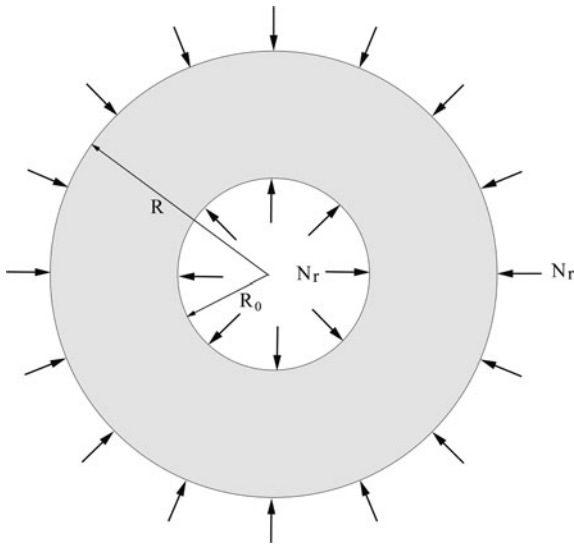


Fig. 1 Circular annular plate under uniform compression

$$\frac{\partial^2 M_{xx}}{\partial x^2} + 2 \frac{\partial^2 M_{xy}}{\partial x \partial y} + \frac{\partial^2 M_{yy}}{\partial y^2} + q + \frac{\partial}{\partial x} \left(N_{xx} \frac{\partial w}{\partial x} \right) + \frac{\partial}{\partial x} \left(N_{xy} \frac{\partial w}{\partial y} \right) + \frac{\partial}{\partial y} \left(N_{yy} \frac{\partial w}{\partial y} \right) + \frac{\partial}{\partial y} \left(N_{xy} \frac{\partial w}{\partial x} \right) = 0 \quad (6c)$$

For uniform radial compression (Fig. 1), we have:

$$N_{xx} = N_r, \quad N_{yy} = N_r, \quad N_{xy} = 0 \quad (7)$$

Here N_r is the compression load as shown in Fig. 1.

Substituting Eqs. (7) into Eqs. (6a)–(6c) yields the governing equation for the buckling analysis of the uniform radial compression of the circular annular plate as in Eq. (8) [1, 29, 32]:

$$\left[D - N_r \mu^2 \right] \nabla^4 w + N_r \nabla^2 w = 0 \quad (8)$$

By some simplifications, Eq. (8) yields the following equation:

$$\left[1 - \frac{\Omega}{R^2} \mu^2 \right] \nabla^4 w + \Omega \nabla^2 w = 0 \quad (9)$$

Here $\Omega = \frac{N_r R^2}{D}$ is the non-dimensional buckling load. The aim of the future attempts is to obtain the non-dimensional buckling load.

3 Finite difference method

As the axisymmetric circular annular nano-plate is tended to study, so the Laplacian operator in polar coordinate could be expressed as follow:

$$\nabla^2 = \frac{d^2}{dr^2} + \frac{1}{r} \frac{d}{dr} \quad (10)$$

Substituting Eq. (10) into Eq. (9) yields the governing equation as follow:

$$\left(1 - \frac{\Omega}{R^2} \mu^2 \right) \left[\frac{d^4 w}{dr^4} + \frac{2}{r} \frac{d^3 w}{dr^3} - \frac{1}{r^2} \frac{d^2 w}{dr^2} + \frac{1}{r^3} \frac{dw}{dr} \right] + \Omega \left(\frac{d^2 w}{dr^2} + \frac{1}{r} \frac{dw}{dr} \right) = 0 \quad (11)$$

Two cases have been studied in this paper: solid disk and circular annular one which will be presented in Sects. 3.1 and 3.2 respectively.

The derivatives of w in the k -th grid point can be explained as Eq. (12) to Eq. (15):

$$\frac{dw}{dr} = \frac{1}{2h} (w_{k+1} - w_{k-1}) \quad (12)$$

$$\frac{d^2 w}{dr^2} = \frac{1}{h^2} (w_{k+1} - 2w_k + w_{k-1}) \quad (13)$$

$$\frac{d^3 w}{dr^3} = \frac{1}{2h^3} (w_{k+2} - 2w_{k+1} + 2w_{k-1} - w_{k-2}) \quad (14)$$

$$\frac{d^4 w}{dr^4} = \frac{1}{h^4} (w_{k+2} - 4w_{k+1} + 6w_k - 4w_{k-1} + w_{k-2}) \quad (15)$$

Here h is the distance between two grid points and subscript of w denotes the point number. Substituting Eqs. (12)–(15) into Eqs. (3a)–(3c) yields:

$$\begin{aligned} & \frac{1}{h^3} \left(1 - \frac{\Omega}{R^2} \mu^2 \right) \left(\frac{1}{h} + \frac{1}{r} \right) w_{k+2} + \frac{1}{h} \left[\left(1 - \frac{\Omega}{R^2} \mu^2 \right) \left(\frac{1}{2r^3} - \frac{1}{r^2 h} - \frac{2}{r h^2} - \frac{4}{h^3} \right) + \Omega \left(\frac{1}{h} + \frac{1}{2r} \right) \right] w_{k+1} \\ & + \frac{1}{h^2} \left[\left(1 - \frac{\Omega}{R^2} \mu^2 \right) \left(\frac{6}{h^2} + \frac{2}{r_k^2} \right) - 2\Omega \right] w_k + \frac{1}{h} \left[\left(1 - \frac{\Omega}{R^2} \mu^2 \right) \left(-\frac{1}{2r^3} - \frac{1}{r^2 h} + \frac{2}{r h^2} - \frac{4}{h^3} \right) \right. \\ & \left. + \Omega \left(\frac{1}{h} - \frac{1}{2r} \right) \right] w_{k-1} + \frac{1}{h^3} \left(1 - \frac{\Omega}{R^2} \mu^2 \right) \left(\frac{1}{h} - \frac{1}{r} \right) w_{k-2} = 0 \end{aligned} \quad (16)$$

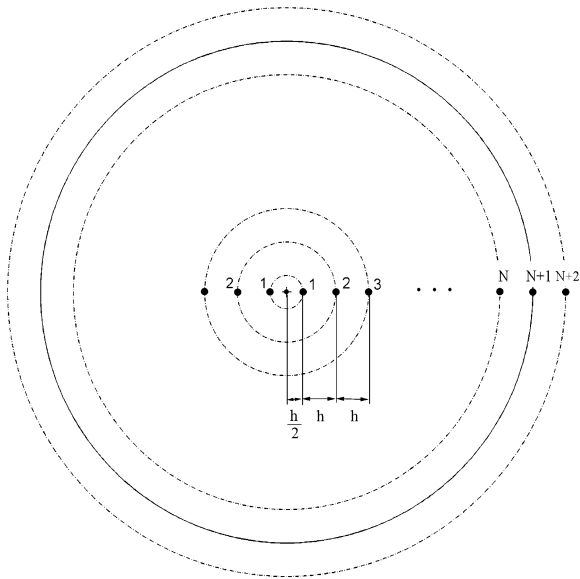


Fig. 2 Grid points for the axisymmetric solid disk

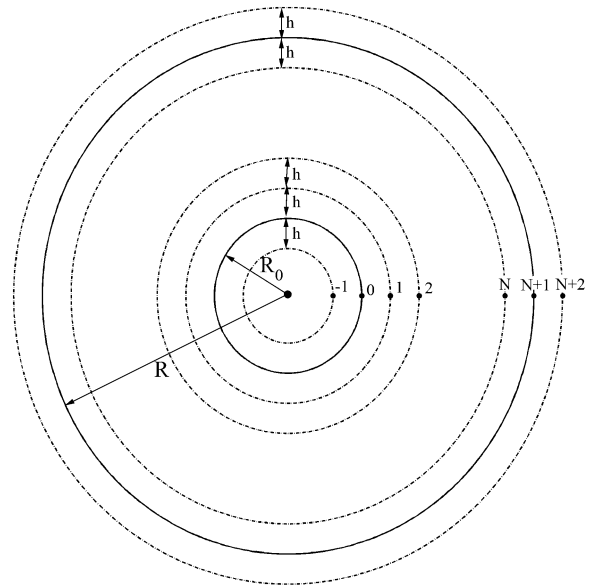


Fig. 3 Grid points for the axisymmetric circular annular plate

3.1 Solid disk

Because of the singularity of the governing equation (11) in the center of the plate, suitable grid should be chosen to repel the singularity. As shown in Fig. 2, the half-intenerated grid has been chosen according to the following equation [33]:

$$r_i = \left(i - \frac{1}{2}\right)h \tag{17}$$

Here $h = \frac{2R}{2N+1}$ and N is the number of interior grid points as shown in Fig. 2. Notice that the value of w_{N+1} and w_{N+2} should be assessed according to the boundary conditions which will peruse in Sect. 3.3.

3.2 Circular annular plate

Figure 3 shows the grid for the circular annular plate which h is the distance between two grid points and is calculated as follow:

$$h = \frac{R - R_0}{N + 1} \tag{18}$$

Here N is the number of interior grid points as shown in Fig. 3. Notice that the values of w_{-1} , w_0 , w_{N+1} and w_{N+2} should be assessed according to the boundary conditions as peruse in next subsection.

3.3 Boundary conditions

In this paper clamp and simply supported boundary conditions have been surveyed at the inner and outer edges. In this section we would assess the values of w_{-1} , w_0 , w_{N+1} and w_{N+2} which are necessary for solving the differential equation (8).

3.3.1 Clamped boundary condition

The clamped boundary condition could be expressed as follows:

$$w = 0, \quad \frac{dw}{dr} = 0 \tag{19}$$

Using the above conditions at inner and outer clamped edges yields:

$$\begin{aligned} w_0 = 0, & \quad w_{-1} = w_1 \\ w_{N+1} = 0, & \quad w_{N+2} = w_N \end{aligned} \tag{20}$$

3.3.2 Simply supported edge

For the simply supported edge the relations are as follow:

$$w = 0, \quad M_r = 0 \tag{20}$$

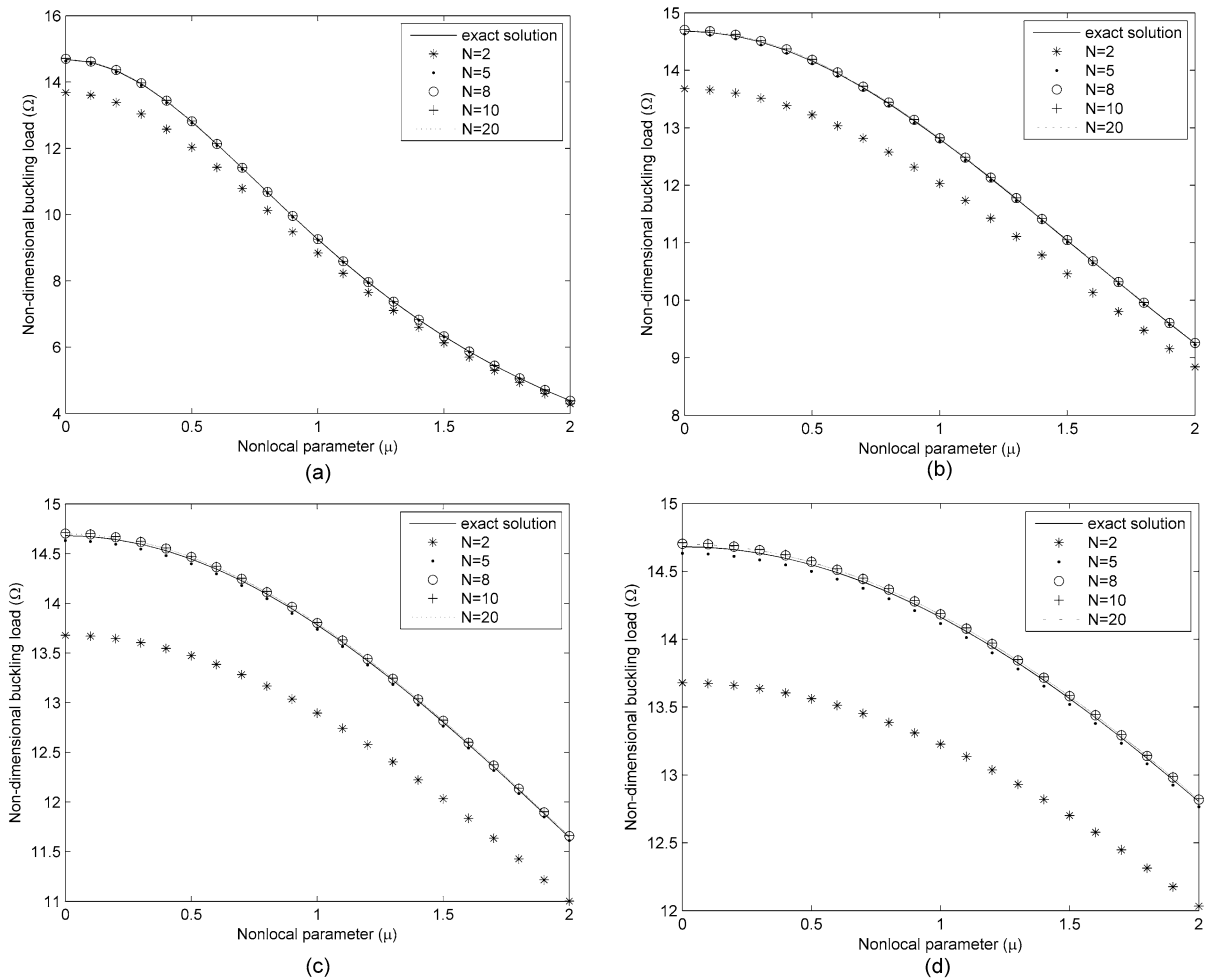


Fig. 4 Change of non-dimensional buckling load with nonlocal parameter for clamped edge and (a) $R = 5$ nm, (b) $R = 10$ nm, (c) $R = 15$ nm, (d) $R = 20$ nm

These conditions yield the following expressions:

$$\begin{aligned}
 w_0 = 0, \quad w_{-1} &= \frac{h\nu - 2R_0}{h\nu + 2R_0} w_1 \\
 w_{N+1} = 0, \quad w_{N+2} &= \frac{h\nu + 2R}{h\nu - 2R} w_N
 \end{aligned}
 \tag{21}$$

4 Solution procedure

Using Eq. (16) in each interior grid point and substituting from the corresponding boundary conditions for w_{-1} , w_0 , w_{N+1} and w_{N+2} , yield N equation contains N unknowns which could be shown as follows:

$$\mathbf{A}\mathbf{w} = 0
 \tag{22}$$

Here A is a square matrix with N rows and N columns and a_{ij} is the coefficient of the w_j in the governing equation of w_i . The evident solution for the system of Eqs. (22) yields the following equation:

$$\det(A) = 0
 \tag{23}$$

Solution of Eq. (23) yields the non-dimensional buckling load in mode number 1 to N .

5 Numerical results and discussion

A MATLAB program has been developed to solve Eq. (23) and to obtain the non-dimensional buckling load for each combination of the boundary conditions and the nonlocal parameter. Let divide the numerical

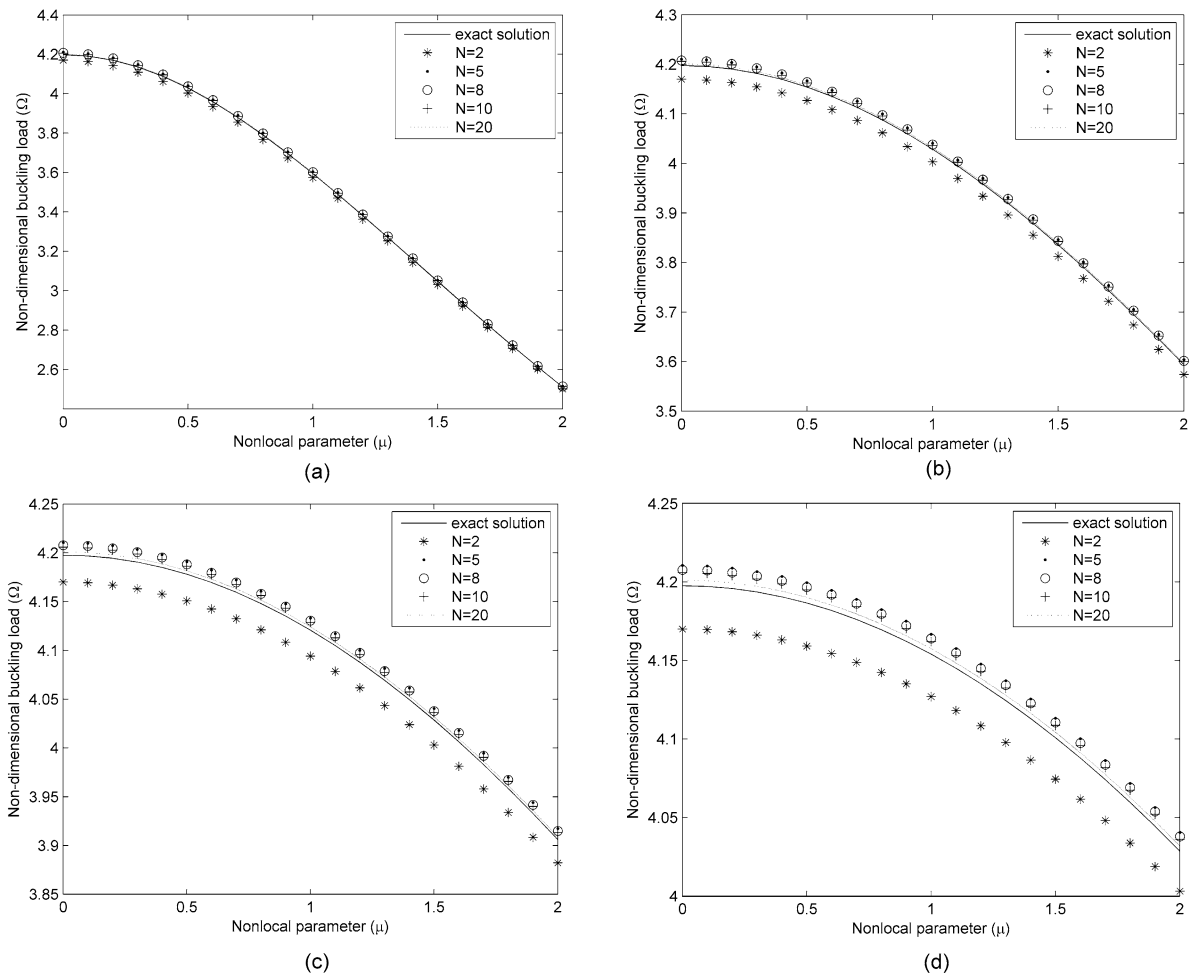


Fig. 5 Change of non-dimensional buckling load with nonlocal parameter for simply-supported edge and (a) $R = 5$ nm, (b) $R = 10$ nm, (c) $R = 15$ nm, (d) $R = 20$ nm

results in two categories one concentrated on the solid disk and another on circular annular one.

5.1 Solid disk

As observed in the literatures the exact solution of the first mode non-dimensional buckling load of a solid disk with clamped and simply-supported edge could be explained as Eqs. (24) and (25) respectively [29]:

$$\Omega = \frac{14.6819}{1 + 14.6819 \frac{\mu^2}{R^2}} \tag{24}$$

$$\Omega = \frac{4.1976}{1 + 4.1976 \frac{\mu^2}{R^2}} \tag{25}$$

Figures 4 and 5 show change of the first mode non-dimensional buckling load (Ω) with nonlocal param-

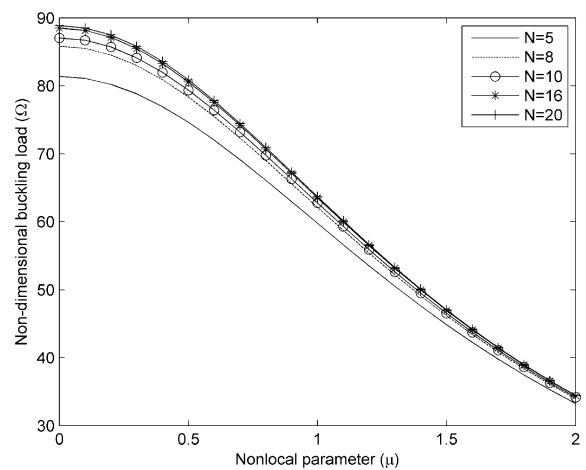


Fig. 6 The effect of the number of internal grids (N) on the non-dimensional load to find the suitable value of N for clamped-clamped boundary condition

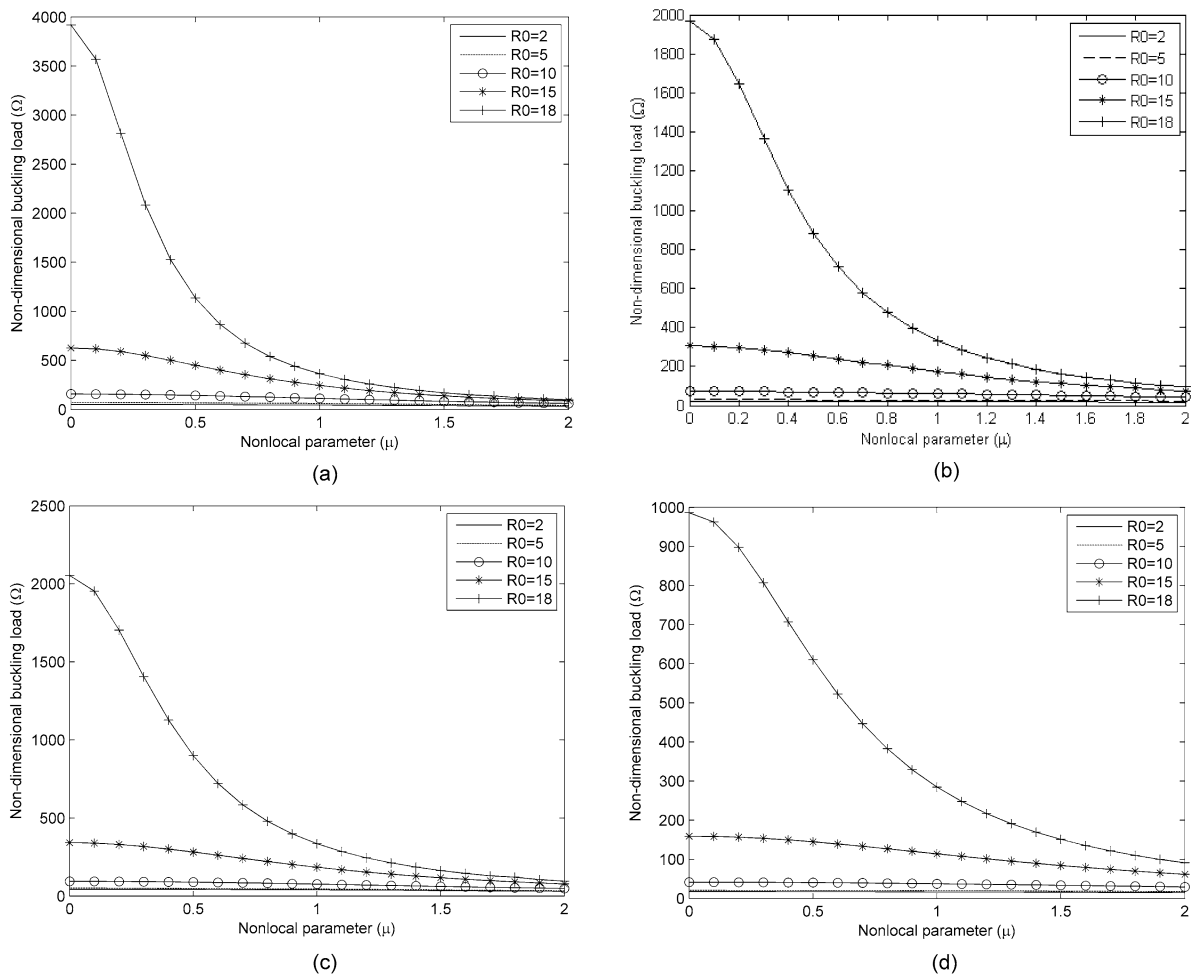


Fig. 7 Change of non-dimensional buckling load with nonlocal parameter for $R = 20$ and (a) C–C, (b) C (inner)–SS (outer), (c) SS (inner)–C (outer), (d) SS–SS (C = Clamped and SS = Simply supported)

eter for several values of number of interior grids (N) for clamped and simply supported boundary conditions respectively. As the radius of the plate increase the number of grid points which is necessary to obtain acceptable results increase. In all cases $N > 5$ presents acceptable results which are in good agreement with those from literature [29].

5.2 Circular annular plate

To have authentic results in each case first the non-dimensional buckling load has been obtained for several value of N while the results variation is slight. Figure 6 shows an example of such verifications. It observed that $N > 16$ yields acceptable results so $N = 20$ has been used in all cases.

Figure 7 shows changes of the non-dimensional buckling load with nonlocal parameter for several values of inner radius (R_0) and fixed outer radius. In all combination of boundary conditions the non-dimensional buckling load increases while the inner radius increased. As another result by increasing of nonlocal parameter the difference between non-dimensional buckling loads of various R_0 s extremely decreased. In another word for greater values of nonlocal parameter the effects of inner radius is slight. (Notice that the pattern of explanation of boundary conditions is as: inner edge boundary-outer edge boundary.)

Figure 8 depicts the effects of the boundary conditions on the non-dimensional buckling load. The plates with C–C boundary conditions have the largest non-dimensional buckling load and SS–SS boundary con-

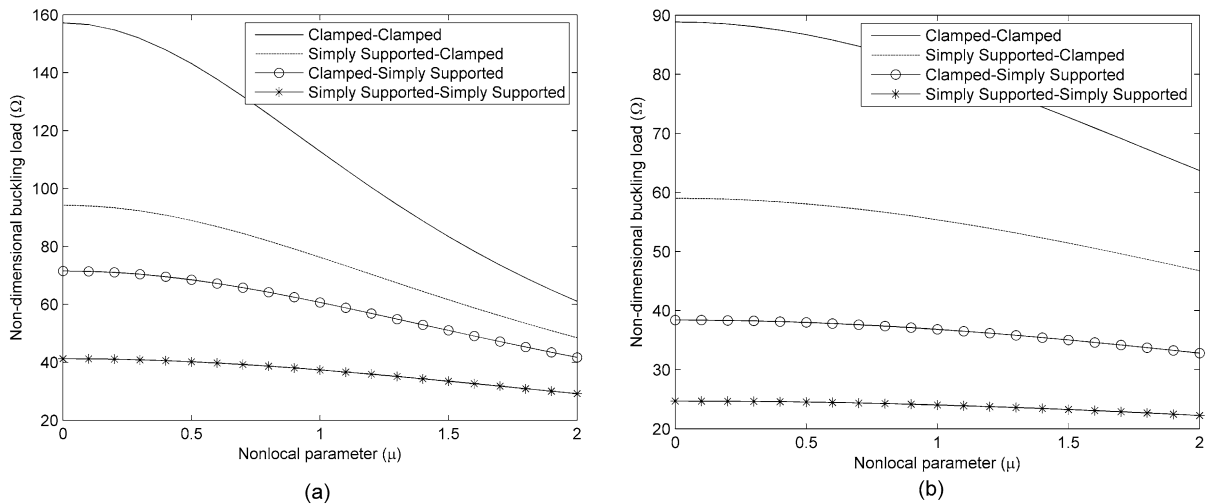


Fig. 8 Change of non-dimensional buckling load with nonlocal parameter for various combination of boundary conditions and (a) $R = 20$, $R_0 = 10$, (b) $R = 30$, $R_0 = 10$

dition yields the smallest one. It is necessary to mention that the non-dimensional buckling load of a SS–C plates is greater than C–SS ones.

6 Conclusion

The governing equation of buckling of circular annular plates has been derived using non-local theory. The half integrated grid in cylindrical coordinate has been chosen to obtain the non-dimensional buckling load. The non-dimensional buckling load of solid disks under clamped and simply supported boundary conditions has been obtained and compared with those from the literatures which are in good agreement. The buckling analysis of the circular annular plates has been surveyed and the effects of the non-local parameter, outer and inner radii and boundary conditions have been studied. Results show the effect of inner radius in large nonlocal parameters is slight. Also plates with clamped-clamped boundary condition have the largest non-dimensional buckling load while simply supported-simply supported have the smallest one. The non-dimensional buckling load of a simply support-Clamped plates is greater than Clamped-simply support ones.

References

- Aksencer T, Aydogdu M (2011) Levy type solution method for vibration and buckling of nanoplates using nonlocal elasticity theory. *Physica E* 43:954–959
- Liu C, Rajapakse RKND (2010) Continuum models incorporating surface energy for static and dynamic response of nanoscale beams. *IEEE Trans Nanotechnol* 9(4):422–431
- Wang GF, Feng XQ (2009) Timoshenko beam model for buckling and vibration of nanowires with surface effects. *J Phys D, Appl Phys* 42:155411
- Farshi B, Assadi A, Alinia-ziazi A (2010) Vibration characteristics of circular nanoplates. *Appl Phys Lett* 96:093105
- Fu Y, Zhang J (2011) Size-dependent pull-in phenomena in electrically actuated nanobeams incorporating surface energies. *Appl Math Model* 35(2):941–951
- Fu Y, Zhang J, Jiang YJ (2010) Influences of the surface energies on the nonlinear static and dynamic behaviors of nanobeams. *Physica E* 42(9):2268–2273
- Sharma JN, Grover D (2011) Thermoelastic vibrations in micro-/nano-scale beam resonators with voids. *J Sound Vib* 330:2964–2977
- Bar On B, Altus E (2011) Effects of local surface residual stresses on the near resonance vibrations of nano-beams. *J Sound Vib* 330:652–663
- Bar On B, Altus E (2012) Clamped nano-beams as adsorption induced sensors: linear and non-linear effects. *Probab Eng Mech* 28:11–17
- Tylikowski A (2011) Stochastic instability via nonlocal continuum mechanics. *Probab Eng Mech* 26:76–80
- Mohammadi B, Ghannadpour SAM (2011) Energy approach vibration analysis of nonlocal Timoshenko beam theory. *Procedia Eng* 10:1766–1771
- Hu Y-G, Liew KM, Wang Q (2012) Modeling of vibrations of carbon nanotubes. *Procedia Eng* 31:343–347
- Yang Y, Zhang L, Lim CW (2011) Wave propagation in double-walled carbon nanotubes on a novel analytically nonlocal Timoshenko-beam model. *J Sound Vib* 330:1704–1717
- Lu P, He LH, Lee HP, Lu C (2006) Thin plate theory including surface effects. *Int J Solids Struct* 43:4631–4647
- Sheng H, Li H, Lu P, Xu H (2010) Free vibration analysis for micro-structures used in MEMS considering surface effects. *J Sound Vib* 329(2):236–246

16. Assadi A, Farshi B, Alinia-ziazi A (2010) Size dependent dynamic analysis of nanoplates. *J Appl Phys* 107:124310
17. Narendar S, Gopalakrishnan S (2012) Temperature effects on wave propagation in nanoplates. *Composites. Part B* 43:1275–1281
18. Arash B, Wang Q, Liew KM (2012) Wave propagation in graphene sheets with nonlocal elastic theory via finite element formulation. *Comput Methods Appl Mech Eng* 223–224:1–9
19. Assadi A, Farshi B, Alinia-ziazi A (2010) Vibration characteristics of circular nanoplates. *J Appl Phys* 108(2):074312
20. Behfar K, Naghdabadi R (2005) Nanoscale vibrational analysis of a multi-layered graphene sheet embedded in an elastic medium. *Compos Sci Technol* 65:1159–1164
21. Murmu T, Pradhan SC (2010) Small scale effect on the free in-plane vibration of nanoplates by nonlocal continuum model. *Physica E* 41(8):1628–1633
22. Murmu T, Pradhan SC (2009) Vibration analysis of nanoplates under uniaxial prestressed conditions via nonlocal elasticity. *J Appl Phys* 106:104301
23. Lin RM (2012) Nanoscale vibration characteristics of multi-layered graphene sheets. *Mech Syst Signal Process* 29:251–261
24. Huang DW (2008) Size-dependent response of ultrathin films with surface effects. *Int J Solids Struct* 45(2):568–579
25. Babaei H, Shahidi AR (2010) Small-scale effects on the buckling of quadrilateral nanoplates based on nonlocal elasticity theory using the Galerkin method. *Arch Appl Mech* 81(8):1051–1062
26. Pradhan SC, Murmu T (2009) Small scale effect on the buckling of single-layered graphene sheets under biaxial compression via nonlocal continuum mechanics. *Comput Mater Sci* 47:268–274
27. Sakhaee-Pour A (2009) Elastic buckling of single-layered graphene sheet. *Comput Mater Sci* 45:266–270
28. Narendar S (2011) Buckling analysis of micro-/nano-scale plates based on two-variable refined plate theory incorporating nonlocal scale effects. *Compos Struct* 93:3093–3103
29. Farajpour A, Mohammadi M, Shahidi AR, Mahzoon M (2011) Axisymmetric buckling of the circular graphene sheets with the nonlocal continuum plate model. *Physica E* 43:1820–1825
30. Nabian A, Rezazadeh G, Derafshi M, Tahmasebi A (2008) Mechanical behavior of a circular micro plate subjected to uniform hydrostatic and non-uniform electrostatic pressure. *Microsyst Technol* 14:235–240
31. Heireche H, Tounsi A, Benzair A, Maachou M, Adda Bedia EA (2008) Nonlocal elasticity effect on vibration characteristics of protein microtubules. *Physica E* 40:2791–2799
32. Assadi A, Farshi B (2011) Size dependent stability analysis of circular ultrathin films in elastic medium with consideration of surface energies. *Physica E* 43:1111–1117
33. Mohanty RK (2000) A fourth-order finite difference method for the general one-dimensional nonlinear bi-harmonic problems of first kind. *J Comput Appl Math* 114:275–290